Kinetics of Crystallization and Crystal Growth of Nanocrystalline Anatase in Nanometer-Sized Amorphous Titania

Hengzhong Zhang* and Jillian F. Banfield†

Department of Geology and Geophysics, University of Wisconsin−Madison, Madison, Wisconsin 53706

Received February 6, 2002. Revised Manuscript Received June 25, 2002

The kinetics of crystallization and crystal growth of nanocrystalline anatase in amorphous titania (2.5−3 nm) samples in the temperature range 300−400 °C was studied by X-ray powder diffraction (XRD) and transmission electron microscopy (TEM). A kinetic model adopting the Smoluchowski coagulation formulation, combined with our phenomenologically derived model kernels, was used to quantitatively interpret the observed kinetic data. It was revealed that the transformation in the amorphous titania comprises four steps: interface nucleation of anatase on contact areas of amorphous particles, with an activation energy of 147 kJ/mol; crystal growth of anatase by redistribution of atoms from either amorphous particles or smaller anatase crystals onto nanocrystal surfaces, both with an activation energy of 78 kJ/mol; and oriented attachment of adjacent anatase particles that are in appropriate orientations, which is less temperature dependent.

Introduction

Both dry and hydrothermal heat treatments of sol−gel amorphous titania (TiO_2) have been used to produce nanocrystalline titania.[1−5] The properties of the products are determined by the phase composition and the particle size of each phase. For instance, the photocatalytic activity of amorphous titania is negligible;[6] that of nanocrystalline anatase is greater than that of rutile; and that of nanocrystalline rutile increases with decreasing particle size.[7] The phase composition and the particle size evolve as functions of time during heat treatment. Therefore, investigation of the kinetics of phase transformation and crystal growth in amorphous titania is essential to the production of nanocrystalline titania with the desired properties.

Upon heating, amorphous titania transforms to anatase and then to rutile when the temperature is high enough.[1,5,8−14] Exarhos and Aloi studied the kinetics of the transformation in amorphous titania films deposited on silica substrates.[8] Yanagisawa et al. found that, under hydrothermal conditions, anatase crystals grow first by fast solid-state interaction, followed by a slow dissolution-recrystallization process.[5,12] Inoue et al. determined the crystallization kinetics of amorphous titania gel in air, water, hexane, and methanol.[13] Kinetic data for transformations in the liquid media (not in air) were analyzed with a surface chemical reaction controlled shrinking core model. Ohtani et al. calcined amorphous titania samples nonisothermally from 300 to 800 °C in air (1−3 h).[6] They inferred that each amorphous particle crystallizes into an anatase particle without crystal growth despite experimental data showing that the particle size of anatase changed from ∼25 to ∼35 nm.

Quantitative analysis of the transformation kinetics of amorphous titania to anatase has only been attempted in liquid media under hydrothermal conditions[13] or for titania films.[8] The rate for the transformation of amorphous titania particles in air should be different from that in liquid media, as evidenced by the difference in the observed starting temperature for the transformation (∼370 °C in air and ∼140 °C in liquid media).[13] In this work, we determined the isothermal kinetics of the transformation of amorphous titania to nanocrystalline anatase and the crystal growth of anatase in air in the temperature range 300−400 °C. On the basis of the proposed transformation mechanism, a kinetic model making use of the Smoluchowski coagulation formulization[15] was developed to interpret the kinetic data.

* To whom correspondence should be addressed.
† Current address: Department of Earth and Planetary Science, University of California−Berkeley, Berkeley, California 94720

(1) Zhang, H.; Finnegan, M.; Banfield, J. F. *Nano Lett.* **2001**, *1*, 81.
(2) Yin, H.; Wada, Y.; Kitamura, T.; Kambe, S.; Murasawa, S.; Mori, H.; Sakata, T.; Yanagida, S. *J. Mater. Chem.* **2001**, *11*, 1694.
(3) Yang, J.; Mei, S.; Ferreira, J. M. F. *J. Am. Ceram. Soc.* **2000**, *83*, 1361.
(4) Wang, C. C.; Ying, J. Y. *Chem. Mater.* **1999**, *11*, 3113.
(5) Yanagisawa, K.; Ovenstone, J. *J. Phys. Chem. B* **1999**, *103*, 7781.
(6) Ohtani, B.; Ogawa, Y.; Nishimoto, S. *J. Phys. Chem. B* **1997**, *101*, 3746.
(7) Gao, L.; Zhang, Q. *Scr. Mater.* **2001**, *44*, 1195.
(8) Exarhos, G. J.; Aloi, M. *Thin Solid Films* **1990**, *193/194*, 42.
(9) Bersani, D.; Lottici, P. P.; Braghini, M.; Montenero, A. *Phys. Status Solidi B* **1992**, *170*, K5.
(10) Haro-Poniatowski, E.; Rodriguez-Talavera, R.; Heredia, M. C.; Cano-Corona, O.; Arroyo-Murillo, R. *J. Mater. Res.* **1994**, *9*, 2102.
(11) Yanagisawa, K.; Ioku, K.; Yamasaki, N. *J. Am. Ceram. Soc.* **1997**, *80*, 1303.
(12) Yanagisawa, K.; Yamamoto, Y.; Feng, Q.; Yamasaki, N. *J. Mater. Res.* **1998**, *13*, 825.
(13) Inoue, Y.; Yin, S.; Uchida, S.; Fujishiro, Y.; Ishitsuka, M.; Min, E.; Sato, T. *Br. Ceram. Trans.* **1998**, *97*, 222.
(14) Ovenstone, J.; Yanagisawa, K. *Chem. Mater.* **1999**, *11*, 2770.

10.1021/cm020072k CCC: $22.00
Published on Web 10/01/2002

Experimental Section

Amorphous titania was prepared by hydrolysis of titanium ethoxide [$Ti(OCH_3CH_2)_4$] in water at 0 °C; 1.6 mol of water (29 mL) containing 4 drops of acetic acid (EM Science, NJ) was quickly added to a mixture of 0.1 mol (21 mL) of titanium ethoxide (ACROS Organics, NJ) and 25 mL of ethanol (AAPER Alcohol and Chemical Co., KY). The solution was continuously stirred for 6 min and then allowed to sit without stirring for 30 min. The product was centrifuged at 8000 rpm for 15 min. The separated white TiO_2 product was washed with water. This centrifuge−washing process was repeated three times. The pH value of the final filtrate was ∼5.0. The final product was dried at 70−80 °C for ∼20 h and stored at room temperature for use as the starting material in this study. Hydrolysis of titanium ethoxide at a higher temperature (e.g., 70 °C) for a longer reaction time (e.g., 24 h) results in the formation of nanocrystalline anatase. Nanometer-sized amorphous titania particles form instead of nanocrystalline anatase particles when titania nuclei are generated rapidly but recrystallization is limited by the low temperature and short reaction time.

Kinetic experiments were carried out between 300 and 400 °C with an increment of 25 °C. Starting materials of ∼40 mg each were put into small alumina crucibles and then immersed in an electrical furnace for different lengths of time. The reacted samples were quenched to room temperature in air and then examined by XRD in a continuous scanning mode between $2\theta = 20°$ and $2\theta = 45°$ at the scanning rate of 0.5°/min using a Scintag PADV X-ray diffractometer. A standard addition analytical method was developed to determine the phase composition in a mixture of amorphous titania + anatase. The method involves addition of a certain amount of standard rutile into the mixture (details were published in ref 1). With this method, the lowest anatase content (or the crystallinity percentage) that can be determined is ∼5%. The average particle size of anatase (D) was calculated using the Scherrer equation:[16,17]

$$D = \frac{0.90\lambda}{\text{FWHM} \cos\theta}$$

where λ is the wavelength of Cu Kα radiation (1.5418 Å), 0.90 is the Scherrer constant, θ is the Bragg reflection angle, and fwhm is the full-width at half-maximum intensity of the anatase (101) peak. Relative standard deviations of both the determined phase composition and average particle size are all ∼7%. Selected samples were examined by TEM for microstructure observation using a Philips CM200 high-resolution transmission electron microscope operated at 200 kV.

Figure 1a shows the XRD pattern (curve 3; Cu Kα radiation, 40 mA, 35 kV, 0.4°/min) of the starting amorphous titania material. For comparison, XRD patterns of bulk anatase and 3-nm nanocrystalline anatase particles are also included (curves 1 and 6, respectively). XRD patterns calculated by Debye function analysis (DFA) of 2-nm amorphous titania particles (curve 2; in DFA, the atomic coordinates were obtained by the molecular dynamics simulations described later), perfectly crystalline 2-nm anatase particles (curve 4) as well as perfectly crystalline 3-nm anatase particles (curve 5) are also depicted for comparison. Figure 1a clearly demonstrates that many of the characteristic peaks of the crystalline anatase (e.g., 101, 004, and 200 peaks) cannot be found in the XRD pattern of the amorphous sample. The theoretically calculated XRD pattern of the 3-nm anatase (curve 5) matches the experimental one (curve 6) very well. Even when the crystalline anatase is ultrafine (e.g., 3 nm), its XRD pattern

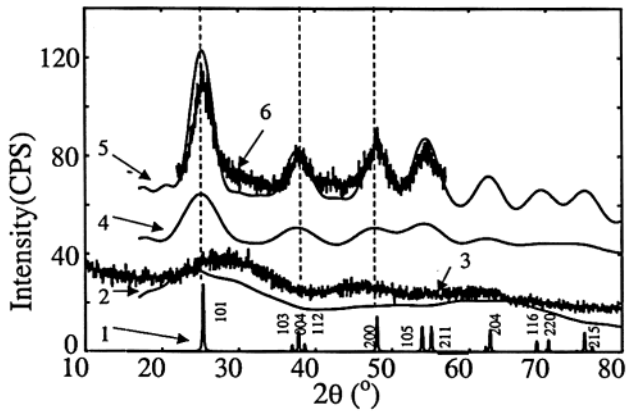

(a)

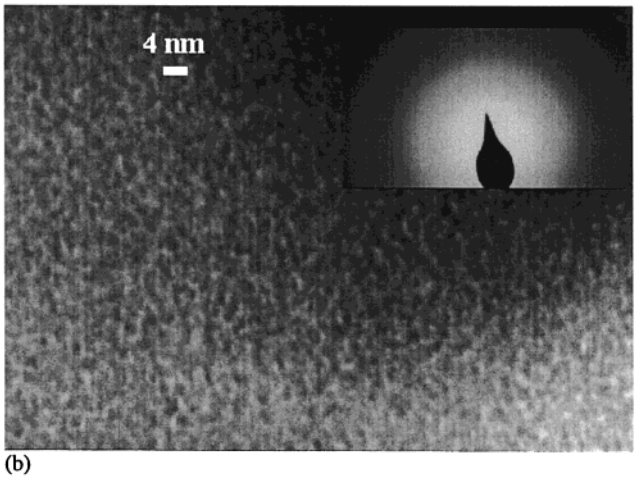

(b)

Figure 1. Experimental XRD pattern (a, curve 3), TEM image, and the SAED pattern (b) of the starting amorphous titania material. For comparison, experimental XRD patterns of bulk anatase (curve 1) and 3-nm nanocrystalline anatase (curve 6) and the XRD patterns by DFA analysis for 2-nm amorphous TiO_2 (curve 2), 2-nm crystalline anatase (curve 4), and 3-nm crystalline anatase (curve 5) are also shown in (a). The CPS unit in (a) only applies to curves 3 and 6.

(curve 6) can still be readily distinguished from that of the amorphous sample (curve 3). Also, curve 3 does not match the XRD patterns of 2−3-nm perfectly crystalline rutile and/or brookite particles by DFA analysis (not shown here). On the other hand, the experimental XRD pattern of the amorphous sample (curve 3) is indeed close to that calculated by DFA for 2-nm amorphous titania particles (curve 2).

Figure 1b shows the TEM image and the selected area electron diffraction (SAED) pattern of the starting amorphous titania material. TEM observation showed that many ultrafine amorphous particles were clumped together to form ∼100-nm diameter spherical aggregates (see Supporting Information). Examination at higher resolution (Figure 1b) revealed the nanometer-sized components of the titania balls. TiO_2 particles are fairly spherical and about 2.5−3 nm in diameter. No lattice fringes, such as those that are readily detected in nanocrystals (even in nanocrystals with stacking faults and disorder), could be found via high-resolution TEM (HRTEM) imaging. The SAED patterns, which sample over micrometer length scales, show highly diffuse rings typical of amorphous materials (Figure 1b and Supporting Information). All of the XRD, SAED, and TEM (HRTEM) findings establish that the starting titania material is amorphous.

The specific surface area of the amorphous titania was determined to be 433 m^2/g by a nitrogen adsorption BET (Brunauer−Emmett−Teller) determination. This surface area is equivalent to an average particle size (diameter) of 3.5 nm,

(15) Dark, R. L. In *International Reviewers in Aerosol Physics and Chemistry*; Hidy, G. M., Brock, J. R., Eds.; Pergamon Press: Oxford, 1972; Vol. 3, p 201.

(16) Jenkins, R.; Snyder, R. L. *Introduction to X-ray Powder Diffractometry*; John Wiley & Sons: New York, 1996; p 90.

(17) (a) Zhang, H.; Banfield, J. F. *J. Mater. Res.* **2000**, *15*, 437. (b) Zhang, H.; Banfield, J. F. *Am. Mineral.* **1999**, *84*, 528.

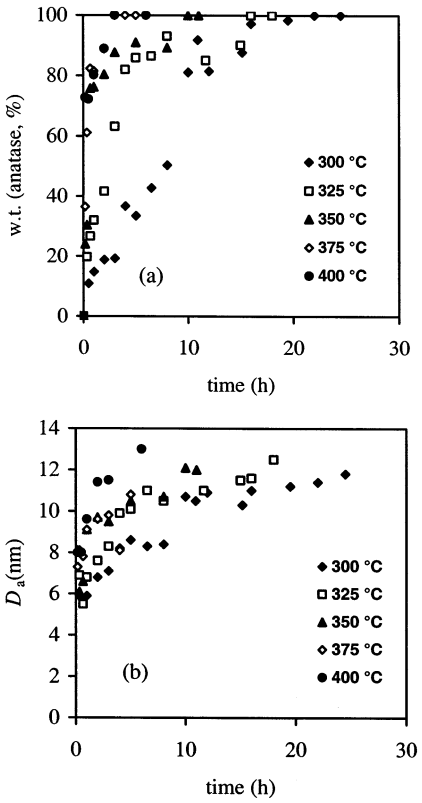

Figure 2. Variation of the anatase content (a) and its average particle size (b) with time due to the transformation of amorphous titania to nanocrystalline anatase at different temperatures.

assuming all amorphous particles are spherical, and the density of the amorphous titania is the same as that of anatase (3.9 g/cm^3), which is close to that of liquid TiO_2 (3.8 g/cm^3) at room temperature by extrapolation.[18] Since some surface areas (e.g., partially coherent interfaces) are inaccessible to the adsorbate, the real size of amorphous particles is probably <3.5 nm. This is consistent with the average grain size of 2.5−3 nm in the TEM image (Figure 1b).

Figure 2 shows kinetic data for the transformation from amorphous titania to anatase. The crystallization of anatase is clearly demonstrated by both the TEM image and the SAED pattern shown in Figure 3a. Usually, for a phase transformation involving bulk nucleation in a solid, there is an induction time (or incubation period) before the transformation proceeds significantly. An incubation period was not observed in our experiment. This may indicate that transformation of amorphous titania to nanocrystalline anatase occurs via interface nucleation; thus, it has a much lower activation energy and can occur at significantly lower temperatures than bulk nucleation.[17]

The average particle size of anatase according to the Scherrer equation by XRD is in good agreement with that determined by TEM observation. This is illustrated for the sample heated at 325 °C for 4 h, where the average particle sizes determined by XRD (Figure 2b) and TEM (Figure 3b) are both ∼10 nm. Close inspection of Figure 3c reveals that many adjacent anatase crystallites are crystallographically oriented with respect to each other. Penn and Banfield and co-workers found that under both hydrothermal and natural conditions, nanocrystal growth can occur via oriented attachment (OA).[19] In this process, crystals adopt crystallographically specific orientations prior to interface elimination. This leads to the formation of single crystals from nanocrystal building blocks. Growth via OA contrasts the general pathway for crystal growth in solution via Ostwald ripening.[20] In the present work, OA was found to occur in dry TiO_2 samples heated in air. Clearly, the TEM observations reported here demonstrate that OA must be taken into account in kinetic modeling of crystal growth under a wide variety of conditions. For further discussion of the OA process (also called oriented aggregation or aggregation-based crystal growth), see ref 21.

Kinetic Model

We tried to fit the kinetic data in Figure 2a for the amorphous to crystalline transformation using a number of published kinetic models. The first is the widely employed Johnson−Mehl−Avrami−Kolmogorov (JMAK) equation:[22,23]

$$\alpha = 1 - \exp(-kt^n) \tag{1a}$$

or

$$\ln[-\ln(1-\alpha)] = \ln k + n \ln t \tag{1b}$$

where k and n are empirical model parameters, α the fraction of transformation, and t the reaction time. Exarhos and Aloi used the JMAK equation to fit their kinetic data for the transformation in amorphous titania films.[8] However, their fitted Avrami exponent (n) is not a constant; rather it is temperature dependent. Figure 4 displays the log−log plot of our experimental data (Figure 2a) according to eq 1b. The Avrami exponents (the slopes of the curves) are not constant, but depend on time, implying the invalidity of the JMAK equation.

Other models tested include standard first-order reaction used to describe the phase transformation from anatase to rutile,[24−26] standard second-order reaction,[24] a contracting spherical interface model,[26−29] a model for nucleation and growth of overlapping nuclei,[26,27] a model for one-dimensional, linear and branching nuclei, and constant growth,[27] and a model for random nucleation and rapid growth.[26,27] Results show that none of the above models are capable of describing the kinetics of the transformation in nanometer-sized amorphous titania samples. In this work, we make use of the Smoluchowski formulization to interpret our kinetic data.

The general Smoluchowski equation has the form of[15,30]

$$\frac{dN_k}{dt} = \frac{1}{2}\sum_{i+j=k} K_{ij}N_iN_j - N_k\sum_{j=1}K_{kj}N_j \quad (i, j, k = 1, 2,...) \tag{2}$$

This equation describes the formation rate of particle k

(18) Dingwell, D. B. *J. Am. Ceram. Soc.* **1991**, *74*, 2718.
(19) (a) Penn, R. L.; Banfield, J. F. *Science* **1998**, *281*, 969. (b) Penn, R. L.; Banfield, J. F. *Am. Mineral.* **1998**, *83*, 1077. (c) Penn, R. L.; Banfield, J. F. *Am. Mineral.* **1999**, *84*, 871. (d) Banfield, J. F.; Welch, S. A.; Zhang, H.; Ebert, T. T.; Penn, R. L. *Science* **2000**, *289*, 751.
(20) Joesten, R. L. In *Review in Mineralogy*; Kerrick, D. M., Ed.; MSA: Washington, DC, 1991; Vol. 26, p 507.
(21) Alivisatos, A. P. *Science* **2000**, *289*, 736.
(22) Christian, J. W. *The Theory of Transformation in Metals and Alloys*, 2nd ed.; Pergamon Press: New York, 1975; p 525.
(23) Borg, R. J.; Dienes, G. J. *The Physical Chemistry of Solids*; Academic Press: Boston, 1992; p 525.
(24) Rao, C. N. R. *Can. J. Chem.* **1961**, *39*, 498.
(25) Suzuki, A.; Kotera, Y. *Bull. Chem. Soc. Jpn.* **1962**, *35*, 1353.
(26) Gennari, F. C.; Pasquevich, D. M. *J. Mater. Sci.* **1998**, *33*, 1571.
(27) Shannon, R. D.; Pask, A. *J. Am. Ceram. Soc.* **1965**, *48*, 391.
(28) Heald, E. F.; Weiss, C. W. *Am. Mineral.* **1972**, *57*, 10.
(29) MacKenzie, K. J. D. *Trans. J. Br. Ceram. Soc.* **1975**, *74*, 77.
(30) Ernst, M. H. In *Fractals in Physics*; Pietronero, L., Tosatti, E., Eds.; Elsevier Science Publishers B.V.: Amsterdam, 1986; p 289.

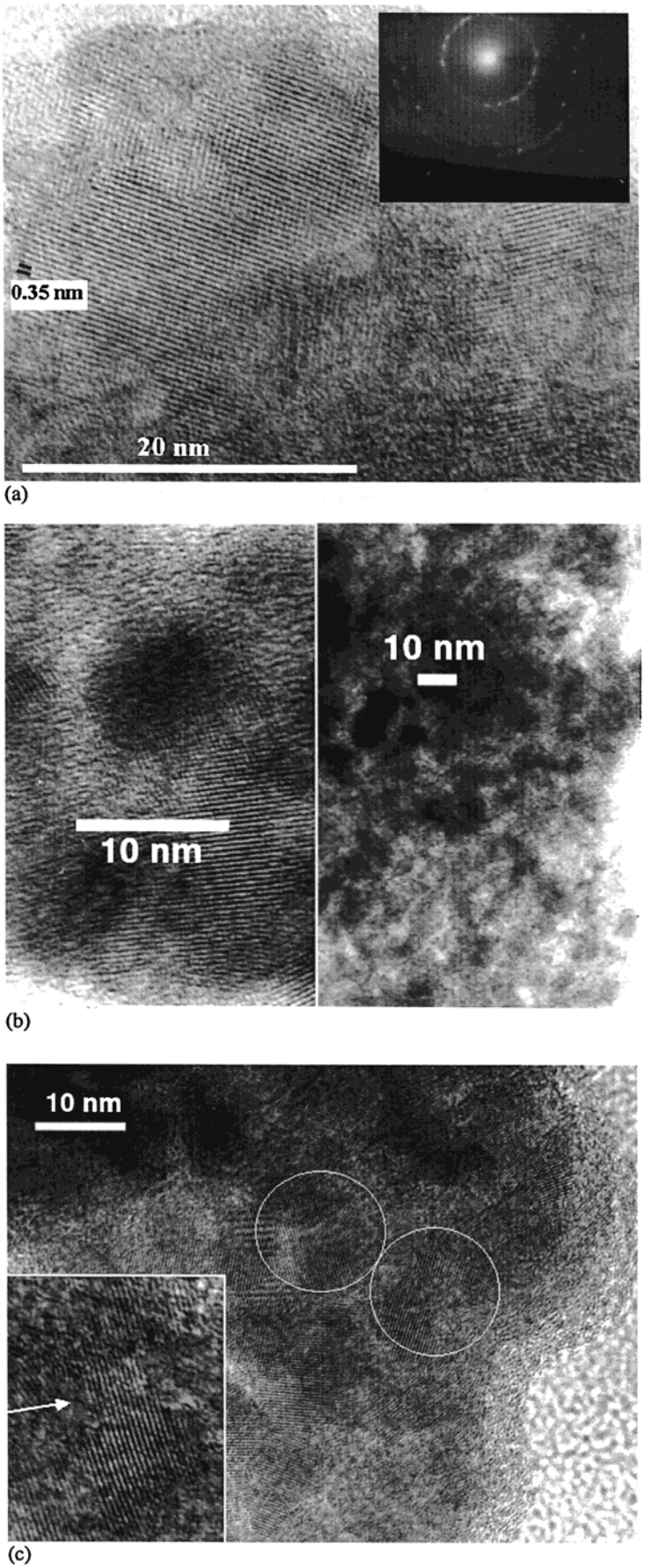

Figure 3. TEM images of samples heated at 325 °C for 2 h (a) and 4 h (b, c). Insert in (a) is a SAED pattern of the sample. Nanocrystalline anatase particles are close to spherical and ~10 nm in diameter (b). The varying contrast and the continuous but not fully straight lattice fringes in the circled areas in (c) suggest that there are anatase particles formed by an orientated attachment. Insert in (c) is a close look on one of the circled areas where the arrow points to the attaching boundary.

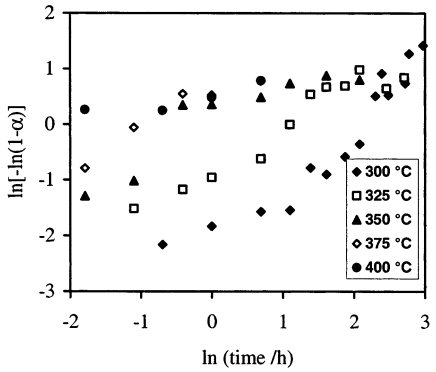

Figure 4. Log−log plot of experimental data shown in Figure 2a. The slopes of these curves range from ~0.5 to 1.3.

through particle aggregation in a system containing many particles. In eq 2, N_i is the number of particles of particle i and K_{ij} is a kinetic constant that is often referred to as the kernel of the Smoluchowski equation. Although the Smoluchowski equation has been used to describe the aggregation (not growth) of nanoparticles in solutions,[31−33] to date it has not been used to describe kinetics of phase transformation accompanying crystal growth.

To understand how nanoparticles undergo transformation from one phase to another, it is necessary to understand their size-dependent structure. It is known that the stable structure of titania is rutile at macroscopic size. But when the particle size of titania is below ~14 nm, anatase is more thermodynamically stable than rutile.[34,35] This arises from the fact that when the particle size decreases to ~14 nm, the molar free energy (J/mol) of rutile becomes higher than that of anatase because rutile has a higher average surface free energy (~1.9 J/m^2) than anatase (~1.3 J/m^2).[35] Usually, an amorphous phase has a lower surface free energy (or surface enthalpy) than its crystalline phase. For example, the surface enthalpy of quartz SiO_2 is 1.0 J/m^2, while that of the amorphous SiO_2 is 0.3 J/m^2 (30% of that of quartz).[36] It is reasonable to assume that the surface free energy of amorphous titania is lower than that of anatase. Accordingly, the 2.5−3-nm amorphous titania particles might be more thermodynamically stable than anatase of the same size, as argued below. If we extrapolate the average particle size of anatase shown in Figure 2b to $t = 0$, we obtain the first detectable particle size of anatase to be 4−5 nm. This size is likely to be larger than that of anatase right after its first formation. If we assume amorphous titania nanoparticles transform to nanocrystalline anatase when the size exceeds 2.5−3 nm, merging two amorphous nanoparticles could trigger the conversion from amorphous titania particles to nanocrystalline anatase particles.

The above argument can be justified by the following simple thermodynamic consideration. First, we assume that the macroscopic structure of nanoamorphous titania can be approximated by that of titania glass formed by quenching molten TiO_2. Then, the difference in the free energy between macroscopic amorphous titania and macroscopic anatase can be calculated to be 32 kJ/mol at 300 K using thermodynamic data from ref 37. In accordance with the thermodynamic analysis given in ref 35, the free energy difference between amorphous titania and anatase at 3 nm is $\Delta G = 32 + (\gamma_{amo} - \gamma_{ana}) \times 10M/(\rho D) = 32 + 68.2(\gamma_{amo} - \gamma_{ana})$ kJ/mol, where γ is the average surface free energy (J/m^2), M the molecular weight of titania, ρ the density of anatase and/or amorphous titania (3.9 g/cm^3), and D the average particle diameter ($D = 3$ nm). If amorphous titania is more stable than anatase at 3 nm, $\Delta G \leq 0$, then $\gamma_{amo} \leq \gamma_{ana} - 32/68.2 = 1.3-0.47 = 0.83$ J/m^2 (i.e., ≤64% of that of anatase). This requirement ($\gamma_{amo} \leq 0.83$ J/m^2) is not extravagant as compared to the case of quartz vs amorphous silica.[36]

The formation of one anatase particle from two amorphous titania particles requires the nucleation and growth of anatase nuclei. For phase transformation from nanoanatase particles to rutile, we have shown previously that at lower temperatures (less than ~600 °C) interface nucleation predominates and this is the rate-controlling step so that the rate of interface nucleation is proportional to the square of the number of nanoparticles.[17] At higher temperatures (>620 °C), surface nucleation of rutile becomes important.[17] However, phase transformation from amorphous titania to anatase was observed at relatively low temperatures in this study (300−400 °C); thus, we assume that interface nucleation also controls the net rate of the merging step of two amorphous titania particles, and the merging rate is proportional to the square of the number of amorphous titania particles (i.e., rate $\propto N_{amor}^2$).

Once anatase is formed through interface nucleation and rapid growth, amorphous titania particles can crystallize onto existing anatase particles by diffusion of atoms, forming bigger anatase particles. The rate of this step should scale with the product of the number of particles of anatase and amorphous titania (i.e., rate $\propto N_{amor}N_{ana}$). Two anatase particles can also merge to form a bigger anatase particle by diffusion of atoms. The rate of this step should scale with the product of the numbers of anatase particles of each size (i.e., rate $\propto N_{ana,size1}N_{ana,size2}$).

On the basis of the above considerations, the following kinetic mechanism is proposed:

(1) Anatase can nucleate during atomic rearrangements that occur at the interface between adjacent amorphous titania particles. Once anatase nucleates, rapid growth at the surface converts the two amorphous particles to a single anatase crystal. Thus,

$$2A_{amor} \rightarrow A_2 \qquad (3)$$

In the above reaction, A_{amor} stands for an amorphous particle and A_2 for an anatase particle formed by merging two amorphous particles. A_{amor} is considered

(31) Lichtenfeld, H.; Knapschinsky, L.; Sonntag, H.; Shilov, V. *Colloids Surf. A* **1995**, *104*, 313.
(32) Gardner, K. H.; Theis, T. L.; Young, T. C. *Colloids Surf. A* **1998**, *141*, 237.
(33) Privman, V.; Goia, D. V.; Park, J.; Matijevic, E. *J. Colloid Interface Sci.* **1999**, *213*, 36.
(34) Gribb, A. A.; Banfield, J. F. *Am. Mineral.* **1997**, *82*, 2, 717.
(35) Zhang, H.; Banfield, J. F. *J. Mater. Chem.* **1998**, *8*, 2073.
(36) Iler, R. K. *The Chemistry of Silica*: *Solubility, Polymerization, Colloid and Surface Properties, and Biochemistry*; John Wiley & Sons: New York, 1979.
(37) Barin, I.; Knacke, O. *Thermochemical Properties of Inorganic Substances*; Springer-Verlag: Berlin, 1973.

as the primary particle in the Smoluchowski eq 2, that is, a particle whose index number $i = 1$. Note that the notation for reaction 3 (and reactions 4 and 5 below) does not have the meaning of a molecular reaction: the coefficient prior to a participant particle is the number of particles of that type involved in the step written, rather than the number of moles as in a molecular reaction.

The rate of the above step, expressed as the increase in the number of the A_2 particles per unit time, is $K_{11}N_1^2$ where K_{11} is the kernel for this step (subscript 11 means amorphous−amorphous interaction). In effect, K_{11} is the kinetic constant for the interface nucleation of anatase.

(2) The growth of anatase particle (index $= 1 + j$) by redistribution of atoms from an amorphous titania particle onto an existing anatase particle (index $= j$):

$$A_{amor} + A_j \rightarrow A_{1+j} \tag{4}$$

The rate of the above step, expressed as the increase in the number of the A_{1+j} particles per unit time, is $K_{1j}N_1N_j$ where K_{1j} is the kernel for this step ($j \geq 2$).

(3) Formation of an anatase particle (index $= i + j$) by redistribution of atoms from an anatase particle (index $= i$) onto another anatase particle (index $= j$):

$$A_i + A_j \rightarrow A_{i+j} \tag{5}$$

The rate of the above step, expressed as the increase in the number of the A_{i+j} particles per unit time, is $K_{ij}N_iN_j$ where K_{ij} is the kernel for this step ($i, j \geq 2$).

In general, the magnitude of the kernel K_{ij} depends on the masses (or volumes) of the two interacting particles i and j and thus is a function of the indices i and j. In the description of aggregation of small particles in a solution, a number of kernels that are pertinent only to the specified mechanisms have been derived.[30] Forms of kernels for crystallization of nanoparticles, K_{1j} and K_{ij}, are not available. They are derived using a phenomenological approach in the following section. In the treatment, all nanoparticles are considered to be spherical.

The thermodynamic driving force for diffusion of atoms involved in reactions 4 and 5 is the spatial gradient of the energy (in the unit of N/mol) between the state before and after the two participating nanoparticles are merged. This is comparable to the diffusion of ions in a solution, where the thermodynamic driving force for diffusion is the spatial gradient of the chemical potential in the space (N/mol).[38] Let ΔE represent the energy change of reactions 4 or 5, D_i the particle size (diameter) of particle i, and D_o the particle size of the primary (amorphous) particles. Since the volume of particle i is i times that of the primary particle, it follows that $D_i = i^{1/3}D_o$. Thus, the energy gradient for reactions 4 or 5 is $\Delta E/[0 - (D_i/2 + D_j/2)] = (-2\Delta E/D_o)/(i^{1/3} + j^{1/3})$, where the spatial separation between the two particles is $D_i/2 + D_j/2$ right before they merge and is zero after they merge. Dividing the thermodynamic driving force by the total mass of the two particles (which is proportional to $i + j$) gives the formal acceleration rate of the merging process. The kernels needed for Smoluchowski eq 2 then can be treated as being proportional to the acceleration rate, that is, kernel $\propto -\Delta E/[(i^{1/3} + j^{1/3}) \times (i + j)]$.

The energy change of reaction 5 comes only from the difference in the particle sizes of the three anatase particles i, j, and $(i + j)$: $\Delta E_5 = \Delta A\gamma$, where ΔA is the change in the molar surface area (m^2/mol). The molar surface area of particle i is $A_i = 6M/(\rho D_i) = 6Mi^{-1/3}/(\rho D_o)$.[35] Thus,

$$\Delta E_5 = \frac{6M\gamma}{\rho D_o}\left[(i+j)^{-1/3} - \frac{i}{i+j}i^{-1/3} - \frac{j}{i+j}j^{-1/3}\right] = \frac{6M\gamma}{\rho D_o}\left[(i+j)^{-1/3} - \frac{i^{2/3}+j^{2/3}}{i+j}\right] \tag{6}$$

Take the values of $M = 79.9$ g/mol, $\rho = 3.9 \times 10^6$ g/m^3, average $\gamma = 1.27$ J/m^2 between 300 and 400 °C for anatase,[35] and $D_o = 3$ nm $= 3 \times 10^{-9}$ m for the primary amorphous titania particles; after inserting these data into eq 6, one obtains

$$\Delta E_5(\text{kJ/mol}) = 52.0\left[(i+j)^{-1/3} - \frac{i^{2/3}+j^{2/3}}{i+j}\right] \tag{7}$$

Since i and $j \geq 2$, $\Delta E_5 < 0$ according to eq 7; thus, merging of two nanoanatase particles is thermodynamically favored.

Similarly, the energy change of reaction 4 is

$$\Delta E_4 = \left[E(\text{anatase},\infty \text{ size}) + \frac{6M\gamma}{\rho D_o}(1+j)^{-1/3}\right] - \frac{1}{1+j}E(\text{amorphous}) - \frac{j}{1+j}\left[E(\text{anatase},\infty \text{ size}) + \frac{6M\gamma}{\rho D_o}j^{-1/3}\right] = -\frac{\Delta E(\text{anatase}, \infty \rightarrow \text{amorphous})}{1+j} + \frac{6M\gamma}{\rho D_o}\left[(1+j)^{-1/3} - \frac{j^{2/3}}{1+j}\right] \tag{8}$$

In eq 8, ΔE(anatase,$\infty \rightarrow$ amorphous) is the difference between the energy of nanometer-sized amorphous titania (2.5−3 nm) and that of the macroscopic anatase. We previously attempted to measure this quantity calorimetrically.[39] A primary result of 24 kJ/mol for this quantity seems inappropriate since the value is even less than the energy difference between bulk titania glass and bulk anatase at room temperature (32 kJ/mol).[37] The measured surface enthalpy of anatase (0.4 J/m^2) might also be underestimated. More elaborate determinations are needed to obtain an accurate value for the quantity. In this work, we utilize the result from molecular dynamics (MD) simulations, which will be published elsewhere.

Interatomic interaction potential functions for Ti−O, Ti−Ti, and O−O by Kim et al.[40] were used in the MD study. MD simulations were carried out at a constant

(38) Atkins, P. *Physical Chemistry*, 5th ed.; W. H. Freeman and Company: New York, 1994; pp 846−849.

(39) Ranade, M. R.; Navrotsky, A.; Zhang, H. Z.; Banfield, J. F.; Elder, S. H.; Zaban, A.; Borse, P. H.; Kulkarni, S. K.; Doran, G. S.; Whitefield, H. J. *PNAS* **2002**, *79* (suppl.2), 6476.

(40) Kim, D. W.; Enomoto, N.; Nakagawa, Z. *J. Am. Ceram. Soc.* **1996**, *79*, 1095.

pressure (10^5 Pa) and a constant temperature of 300, 350, or 400 °C, using MD programs SHELL-DYNAMO[41] and XMD.[42] Each simulation was run at a time step of 2.5 fs for 10 000 steps (25 ps). An original 3-nm anatase structure was fully relaxed during the simulation. The relaxed structure was found to be noncrystalline. The XRD pattern of the relaxed structure calculated by Debye function analysis[43] confirmed that the relaxed structure is in an amorphous state. On the other hand, the XRD pattern by DFA of a MD relaxed structure of an original 3.5-nm anatase particle exhibits characteristic peaks of anatase. These results suggest that the particle size between 3 and 3.5 nm represents the crossover for the reversal of phase stability in amorphous titania and anatase, which supports our previous discussion in an early section. According to the MD simulations, the energy of the 3 nm amorphous titania particle is ~100 kJ/mol higher than that of macroscopic anatase in the temperature range 300−400 °C.

Replacing ΔE(anatase, $\infty \rightarrow$ amorphous) of eq 8 with 100 kJ/mol, one obtains

$$\Delta E_4(\text{kJ/mol}) = -\frac{100}{1+j} + 52.0\left[(1+j)^{-1/3} - \frac{j^{2/3}}{1+j}\right] \quad (9)$$

For all $j \geq 2$, $\Delta E_4 < 0$ according to eq 9.

Since a kernel $\propto -\Delta E/[(i^{1/3} + j^{1/3})(i + j)]$, thus for crystallization reaction 4,

$$K_{1j} = k_{\text{amor}}\left\{\frac{100}{1+j} + 52.0\left[\frac{j^{2/3}}{1+j} - (1+j)^{-1/3}\right]\right\}/ [(1+j^{1/3})(1+j)] \quad (10)$$

where k_{amor} is a constant for all interactions between an amorphous particle and an anatase particle j ($j \geq 2$). For recrystallization reaction 5,

$$K_{ij} = 52.0k_{\text{aa}}\left[\frac{i^{2/3}+j^{2/3}}{i+j} - (i+j)^{-1/3}\right]/ [(i^{1/3}+j^{1/3})(i+j)] + k_{\text{OA}} \quad (11)$$

Here, k_{aa} is a constant for all interactions between anatase particles i and j ($i, j \geq 2$). In eq 11, the contribution to the kernel from the oriented attachment (k_{OA}) has been considered.

Under hydrothermal conditions,[19] the higher the concentration of nanoparticles in the solution, the greater the chance for nanoparticles to collide with each other. Thus, the formation rate of OA in a solution should scale with the concentration of the nanoparticles. Brownian motion and thermal convection may cause nanoparticles to collide, so the temperature should have a marked influence on OA in a solution. For dry titania samples, particle−particle contact must be achieved in a different way for OA to proceed. During the crystallization of amorphous titania, a large number of nanocrystalline anatase particles form in random orientations. Two adjacent anatase particles may happen to be crystallographically oriented with respect to each other; in which case, they may combine to form a single particle that is randomly oriented with respect to its neighbors. This process will continue so long as particles in appropriate orientations are present. Thus, OA can be treated as a random event in dry samples. Its probability should be influenced mainly by sample preparation details, rather than the temperature for amorphous crystallization, though the heat released by OA may exert some influence. Consequently, we treat k_{OA} to be a constant that is valid for all possible $i-j$ particle interactions via OA.

Modeling of Kinetic Data

So far, explicit forms of the model kernels are obtained: K_{11} = constant, K_{1j} described by eq 10, and K_{ij} by eq 11.

Figure 2b indicates that the observed maximum average particle size of anatase is ~13 nm. It is safe to assume that all anatase particles are <21 nm in our kinetic system. Thus, the maximum index needed for Smoluchowski eq 2 is $n = (D_{\max}/D_o)^3 = (21/3)^3 = 343$.

All $i-j$ particle interactions [denoted as (i, j) below] must be constrained by n such that $i + j \leq n$. Thus, all interactions can be enumerated as follows:

(1,1)	(1,2)	(1,3)	(1,4)	... (1,$n-1$)	counts=$n-1$
	(2,2)	(2,3)	(2,4)	... (2,$n-2$)	counts=$n-2-1=n-3$
		(3,3)	(3,4)	... (3,$n-3$)	counts=$n-3-2=n-5$
			(4,4)	... (4,$n-4$)	counts=$n-4-3=n-7$
...					
			(i,i)(i,i+1)	... (i,$n-i$)	counts=$n-i-(i-1)=n+1-2i$
...					
			(170,171)	(170,172) (170,173)	counts=3
				(171,171) (171,172)	counts=2

Then the total number (M) of all possible interacting pairs can be obtained by summing all the counts:

$$M = \sum_{i=1}^{\text{int}(n/2)} (n+1-2i) = \text{int}\left(\frac{n}{2}\right)\left[n - \text{int}\left(\frac{n}{2}\right)\right] \quad (12)$$

where int(x) is the greatest integer function for which the returned value is the greatest integer less than x. For our case, $n = 343$ and $M = 29\,412$.

The initial condition for those equations is that, at the very beginning ($t = 0$), there are only primary amorphous titania particles in the system:

$N_i(t=0) =$
- N_o (initial number of amorphous particles) for i=1 (amorphous titania)
- 0 (initially there are no anatase particles) for 2≤ i ≤343 (anatase particles)

It is impossible to solve 343 coupled differential equations (eq 2) analytically with kernels of the forms of eqs 10 and 11. A numerical method was used to solve these differential equations (see Supporting Information). Giving values for a set of the model parameters (K_{11}, k_{amor}, k_{aa}, and k_{OA}) and the initial number of primary particles (N_o), the number of particles $N_i(t)$ ($i = 1-343$) were simulated at a time step of 0.01 h for a time length of up to $t = 25$ h. Since N_o is unknown, a normalized quantity of $N_o = 1$ was used in the numerical calculation. The actual value of N_o only affects the

(41) Fincham, D. *Shell-Dynamo Reference Manual*; University of Keele: Staffordshire, U.K., 1996.
(42) Rifkin, J. *XMD-Molecular Dynamics Program*; University of Connecticut: Storrs, Connecticut, 2002.
(43) Kazakov, A. V.; Shpiro, E. S.; Voskoboinikov, T. V. *J. Phys. Chem.* **1995**, *99*, 8323.

Table 1. Parameters for the Kinetic Model

temp (°C)	K_{11} (1/h)	k_{amor} (30/h)	k_{aa} (600/h)	k_{OA} (1/h)
300	0.01	1.5	0.24	2.0
325	0.04	3.0	0.6	2.0
350	0.12	5.5	1.1	2.0
375	0.36	9.0	1.8	1.0
400	1.08	18.0	3.6	2.0

relative magnitudes of $N_i(t)$ but does not affect the calculated transformation percentage and the particle size.

The anatase content (or the transformation percentage) can be calculated from

$$\text{w.t.(anatase, \%)} = 100\left(1 - \frac{N_1}{N_o}\right) \qquad (13)$$

And the volume-averaged particle size of anatase can be calculated from

$$D = \frac{\sum_{i=2}^{343} N_i D_i^4}{\sum_{i=2}^{343} N_i D_i^3} = \frac{\sum_{i=2}^{343} N_i (D_o i^{1/3})^4}{\sum_{i=2}^{343} N_i (D_o i^{1/3})^3} = \frac{\sum_{i=2}^{343} i^{4/3} N_i}{\sum_{i=2}^{343} i N_i} D_o \qquad (14)$$

The particle size obtained from eq 14 is comparable to the average particle size determined by XRD using the Scherrer method because the latter reflects the volume-averaged particle size of all particles.[44]

Since there is no analytical solution to the Smoluchowski equation for our kinetic system, it is extremely difficult to do parameter optimization; thus, we used a trial-and-error method to search for suitable model parameters. First, on the basis of pretest of several numerical simulations, each parameter in the kinetic model was allowed to take three levels of values: K_{11} (1/h) = 0.01, 0.1, 1; k_{amor} (30/h) = 0.1, 1, 10; k_{aa} (600/h) = 0.1, 1, 10; and k_{OA} (1/h) = 0, 2.5, 5. Simulations with a combination of any level of a parameter with any level of the rest parameters were computed, generating a total of $3^4 = 81$ simulated results. These results were converted to the anatase percentage and the average particle size data according to eqs13 and 14 and then compared against the experimental data shown in Figure 2 for all five temperatures (300−400 °C). Those sets of parameters that produce closest agreement between the simulated results and the experimental data were chosen for fine-tuning in the following step.

Each parameter obtained from the first step was allowed to deviate from its value to some extent, and the corresponding simulation was done. The simulated results were compared again with the experimental data (Figure 2). The combination of the parameters that exhibits the best coincidence between the simulation and the experimental was taken as the suitable set of model parameters for a given temperature (Table 1).

Figure 5 shows the results of simulations using parameters listed in Table 1, together with a comparison with experimental data. Fairly good agreement between the model results and the experimental data can be seen, except for at 300 °C where there are apparent deviations in the anatase contents at longer reaction times (Figure 5a). Figure 6 shows a comparison between particle size distribution (PSD) of anatase particles measured from TEM images and that calculated from the kinetic model. The model reasonably reproduced the bimodal shape of the PSD curve.

(44) Allen, T. *Particle Size Measurement*; Chapman and Hall: New York, 1997; Vol. 1, p 53.

Discussion and Conclusions

The present kinetic model is able to describe both the transformation percentage and the particle size evolution fairly well within one model, which is a critical test of the model. Other models, such as the JMAK approach and the Ostwald-ripening theory, can only describe the transformation percentage or the particle size evolution individually.

At 300 °C, thermal fluctuation at the interfaces between two contacting amorphous particles may not be high enough to create anatase nuclei. Thus, more than two amorphous titania particles may be able to coarsen to form a bigger amorphous particle. These bigger amorphous particles are metastable with respect to anatase of the same size and should convert to anatase upon further reaction. Merging of three or more amorphous particles was not considered in the current model, which could account for the underestimation of anatase content at longer reaction time at 300 °C (Figure 5a).

Figure 7 shows the influences of the model parameters on the simulated results for the phase transformation and anatase coarsening. The best set of parameters is that for curve 1, which reproduces well the experimental data of both the anatase content and its averaged particle size. When one (or more) parameter deviates from the best set, either the anatase content, the averaged particle size, or both cannot be reproduced well at the same time. This suggests that the best set of parameters is unique. It can also be seen that the rate of the transformation is mainly determined by K_{11} of reaction 3 and k_{amor} of reaction 4. All reactions 3−5, including OA, affect the anatase coarsening appreciably.

Table 1 reveals that, except for k_{OA}, parameters vary with temperature significantly. This is consistent with our assumption that OA is a random event, the rate of which is mainly determined by the product of the numbers of the nanoparticles involved in the OA. For T = 375 °C, we have chosen $k_{OA} = 1$ because the calculated average particle size of anatase at $k_{OA} = 1$ is slightly closer to the experimental one than when $k_{OA} = 2$ as for other temperatures, though the difference in the calculated average particle sizes is <0.5 nm for the two cases. Figure 8 shows the Arrhenius plot of K_{11}, k_{amor}, and k_{aa} between 325 and 400 °C. From the plot, the activation energy $E_a = -2.303 \times 8.314 \times$ slope (kJ/mol). The activation energy for interface nucleation of anatase in amorphous titania particles, $E_a(K_{11}) = 147$ kJ/mol, is almost identical to that reported previously for transformation in amorphous titania films on a substrate (142 kJ/mol)[8] and is also comparable to that for interface nucleation of rutile from nanocrystalline anatase (166 kJ/mol).[17] The activation energy for anatase recrystallization, $E_a(k_{aa}) = 78$ kJ/mol, is the same as that for crystallization of amorphous particles on to existing anatase particles, $E_a(k_{amor})$. This means that the two steps are probably governed by the same atomic

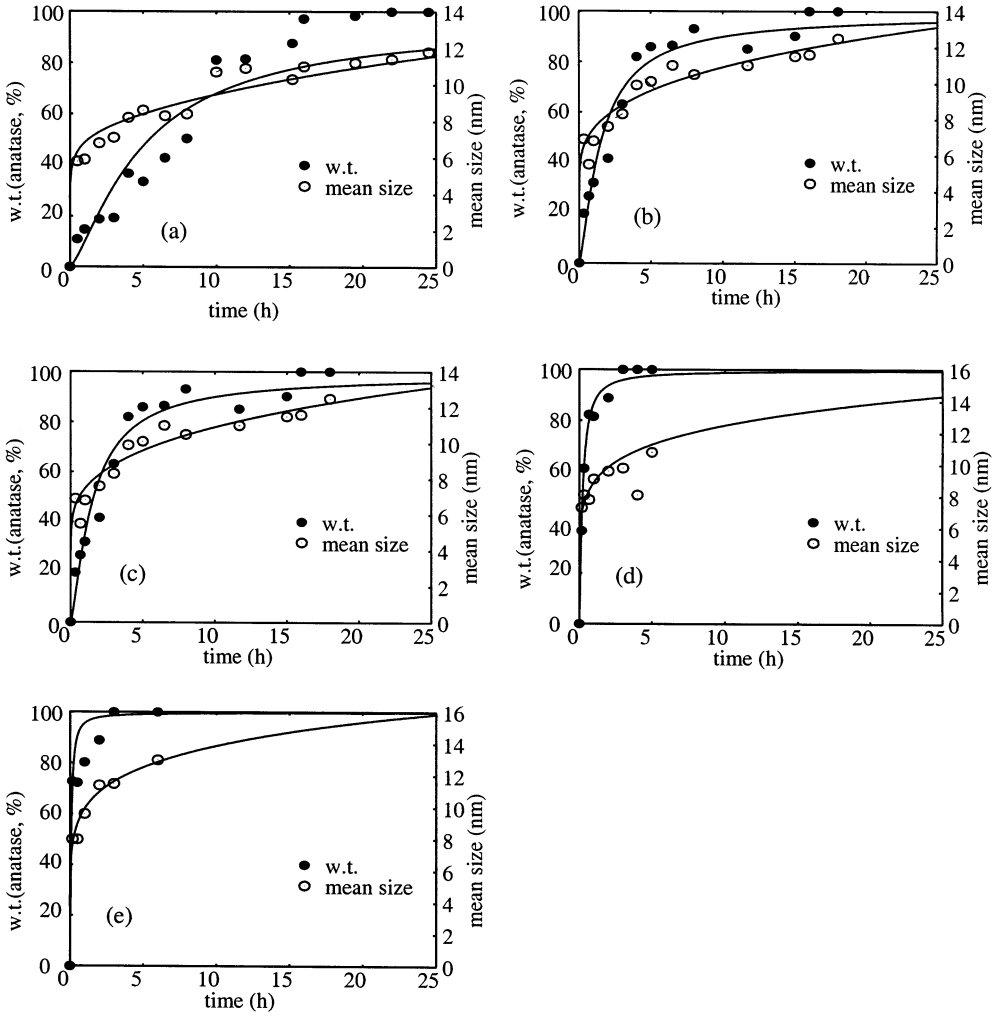

Figure 5. Comparison between simulated results (solid lines) from kinetic model and the experimental data (circles): (a) 300 °C, (b) 325 °C, (c) 350 °C, (d) 375 °C, and (e) 400 °C.

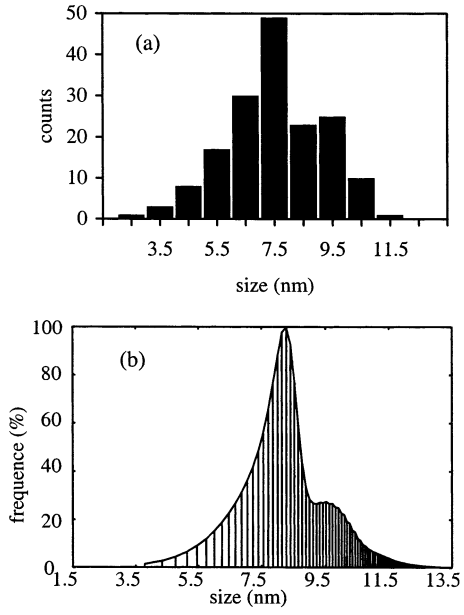

Figure 6. Particle size distribution of anatase particles in the sample heated at 325 °C for 4 h, as measured from TEM images (a) and calculated from the kinetic model (b).

diffusion. The activation energy for anatase recrystallization is also close to that for anatase coarsening, 69 kJ/mol, as reported previously in ref 17. The uncertainty in the activation energy (ΔE) can be estimated from the relative uncertainty ($\Delta k/k$) of the kinetic constant k using $\Delta E = RT(\Delta k/k)$. The $\Delta k/k$ could be calculated from the relative standard deviations (all ~7%) of both the anatase content (w.t.%) and its average particle size (D) in the XRD determination using the error propagation theory if the analytical relationship between k and w.t. % and D were known. However, this analytical relationship is not available since the Smoluchowski eq 2 could not be solved analytically for the kinetic model presented in the present work. Nevertheless, it is expected that the relative uncertainty of a kinetic constant k due to the error propagation from the experimental determination is less than 2 × 7%. Accordingly, the maximum uncertainty in the activation energy $\Delta E = 8.314 \times 673 \times 2 \times 7\% \times 10^{-3} = 0.8$ kJ/mol. Even if there is 100% uncertainty in the k, the $\Delta E = 8.314 \times 673 \times 100\% \times 10^{-3} = 5.6$ kJ/mol, which is still small as compared to the absolute value of E_a (78 or 147 kJ/mol).

We present here the first kinetic model that interprets both the crystallization and the crystal growth behavior of nanometer-sized amorphous titania samples. It is based on a devised mechanism that is supported by high-resolution TEM evidence and is able to reproduce the experimental data and yield activation energies for parallel reactions that are consistent with those from

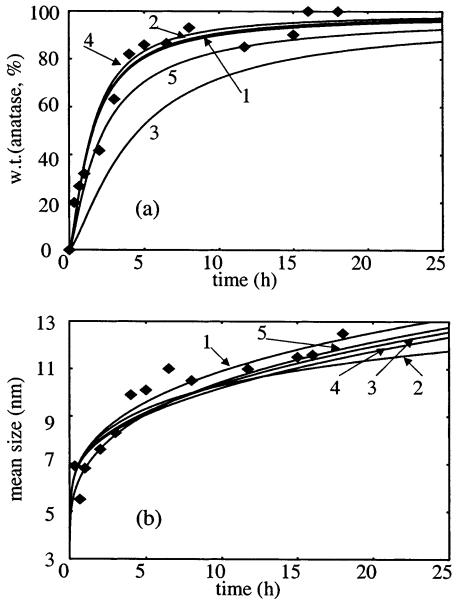

Figure 7. Influence of model parameters on the simulated results (solid lines), with comparison with kinetic data (diamonds) at 325 °C: (a) anatase content vs time; (b) average particle size of anatase vs time. Solid lines: (l) kinetic parameters as in Table 1; (2) parameters as in Table 1 but $k_{OA} = 0$; (3) parameters as in Table 1 but $K_{11} = 0.01$ (1/h); (4) parameters as in Table 1 but $k_{aa} = 0.2$ (600/h); and (5) parameters as in Table 1 but $k_{amor} = 1$ (30/h).

prior studies. The kinetic model presented here can predict not only the phase composition but also the average particle size and the particle size distribution. It should have important implications in the preparation of nanocrystalline particles using amorphous particles as the raw material. This model also provides new insight into how some natural nanoparticles form from their amorphous colloidal aggregates in environments on the Earth and elsewhere.

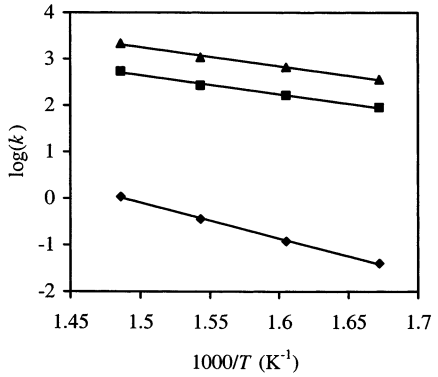

Figure 8. Arrhenius plot of model parameters (diamond, K_{11}; square, k_{amor}; triangle, k_{aa}).

Acknowledgment. We would like to thank Dr. M. R. Ranade for the BET determination, Mr. M. Finnegan for providing an XRD pattern of 3-nm nanocrystalline anatase, Dr. D. Fincham for providing the SHELL-DYNAMO code, and Dr. J. Rifkin for providing the XMD code. Financial support for this study was provided by National Science Foundation Grants EAR-9814333 and EAR-0123967.

Supporting Information Available: Algorithm for the numerical solution of the kinetic model and additional TEM/SAED images (PDF). This material is available free of charge via the Internet at http://pubs.acs.org.

CM020072K